applied optics

Accurate alignment of optical axes of a biplate using a spectroscopic Mueller matrix ellipsometer

Honggang Gu,[1] Xiuguo Chen,[1] Hao Jiang,[1,*] Chuanwei Zhang,[1,2] Weiqi Li,[1] and Shiyuan Liu[1,2]

[1]State Key Laboratory of Digital Manufacturing Equipment and Technology, Huazhong University of Science and Technology, Wuhan 430074, China
[2]Wuhan Eoptics Technology Co. Ltd., Wuhan 430075, China
*Corresponding author: hjiang@hust.edu.cn

Received 26 January 2016; revised 12 April 2016; accepted 12 April 2016; posted 13 April 2016 (Doc. ID 258252); published 12 May 2016

The biplate that consists of two single wave plates made from birefringent materials with their fast axes oriented perpendicular to each other is one of the most commonly used retarders in many optical systems. The internal alignment of the optical axes of the two single wave plates is a key procedure in the fabrication and application of a biplate to reduce the spurious artifacts of oscillations in polarization properties due to the misalignment error and to improve the accuracy and precision of the systems using such biplates. In this paper, we propose a method to accurately align the axes of an arbitrary biplate by minimizing the oscillations in the characteristic parameter spectra of the biplate detected by a spectroscopic Mueller matrix ellipsometer (MME). We derived analytical relations between the characteristic parameters and the misalignment error in the biplate, which helps us to analyze the sensitivity of the characteristic parameters to the misalignment error and to evaluate the alignment accuracy quantitatively. Experimental results performed on a house-developed MME demonstrate that the alignment accuracy of the proposed method is better than 0.01° in aligning the optical axes of a quartz biplate.

OCIS codes: (120.2130) Ellipsometry and polarimetry; (230.5440) Polarization-selective devices; (220.1140) Alignment; (120.0120) Instrumentation, measurement, and metrology; (120.6200) Spectrometers and spectroscopic instrumentation.

http://dx.doi.org/10.1364/AO.55.003935

1. INTRODUCTION

Wave plates made from birefringent materials are indispensable components in many optical systems, such as ellipsometry [1,2], polarimetry [3], interferometry [4], spectroscopy [5], and tomography [6], to modify the polarization state by introducing a phase shift between two orthogonal components of a polarized light. Biplate is one of the typical and most commonly used wave plates, which consists of two single wave plates made from the same material or different materials to make a compound zero-order retarder or an achromatic retarder [7]. During the fabrication of a biplate, the internal alignment of the optical axes of the two single wave plates is one of the key procedures to ensure the fast axes of the single wave plates perpendicular to each other. The misalignment errors in the fast axes of the single wave plates introduce undesirable oscillations in the spectra of optical properties of the biplate, such as the retardance and the fast-axis azimuth [8–12]. These oscillations will further lead to spurious artifacts in the final collected data and degrade the measurement accuracy of the optical systems [13–18]. Therefore, it is of great importance to strictly align the optical axes of the biplate to eliminate these misalignment artifacts and to improve the optical performances of the biplate.

Chenault and Chipman used a rotating sample spectropolarimeter to calibrate the linear retardance, the fast-axis azimuth, and the linear diattenuation of an infrared achromatic wave plate containing misalignment error [10]. Boulbry *et al.* developed an apparatus based on a method of null intensity using a spectral light source to calibrate the fast-axis azimuth spectrum of a misaligned biplate, and they further explained and identified the misalignment error in the biplate [15,18]. Recently, some new techniques have been reported to characterize the misalignment errors in the composite wave plates, including the rotating-compensator reflectance difference spectrometer [5], the rotating-compensator ellipsometer [19], the Mueller matrix ellipsometer (MME) [12], and the three-spectrum method [11]. However, most of these techniques seem difficult to be used for accurate axis alignment of the composite wave plates. In addition, the optical model utilized in some of these methods ignores the optical rotary angle that results from the structure of the misaligned composite wave plates, which prevents them from giving a comprehensive description about the polarization properties of the wave plates.

Although the above methods can calibrate the axis-misalignment errors in wave plates in the applications, the best

way to eliminate the influences of the misalignment errors is to strictly align the single wave plates in the manufacturing process. Existing methods for the axis alignment of biplates can be summarized as choosing a characteristic parameter that is sensitive to the variation of the misalignment errors in biplates and then reducing the oscillations in the characteristic parameter below the limit of detectability by rotating a single wave plate with respect to another one. In the fabrication of a biplate, most of the manufacturers use a null-intensity method to align the optical axes of the single wave plates. In this method, the intensity is chosen as the characteristic parameter to be detected, and the biplate is placed and aligned between two orthogonal polarizers by distinguishing the extinction position. Since the null-intensity method detects the original intensity and relies on the discrimination of the extinction position of the polarizer-biplate-polarizer system, the alignment accuracy is significantly influenced by the environmental noise and the relative azimuths between the polarizers and the biplate. In the published literatures, several advanced techniques have been proposed to align the axes of biplates. Aspnes improved the null-intensity configuration and constructed a straight-through, polarizer-compensator-analyzer ellipsometer to align the axes of an optically active biplate by minimizing the deviations in the azimuths of the polarizer and analyzer [20]. Aspnes's method still requires the extinction condition of the polarizer and the analyzer (i.e., the transmission axis of the polarizer is perpendicular to that of the analyzer), and it is an indirect method since it detects and controls the azimuths of the polarizer and analyzer instead of a characteristic parameter of the biplate compensator. Lee *et al.* further presented a method to align and calibrate an magnesium fluoride (MgF_2) biplate using a straight-through rotating-analyzer (PCA_r) ellipsometer by reducing the high-frequency oscillations in the ellipsometric angles (i.e., the amplitude ratio Ψ_C and the retardance δ_C) of the biplate [21]. However, the PCA_r ellipsometer is sensitive to the polarization error in the detector, and both of the ellipsometric angles have low sensitivity to the misalignment errors compared with the fast-axis azimuth and the rotary angle of a misaligned biplate. In addition, to the best of our knowledge, these reported methods did not evaluate the alignment accuracy and the residual misalignment errors quantitatively due to the lack of analytical relations between the characteristic parameters and the misalignment errors.

The MME has been developed as a powerful tool to characterize samples, which contain anisotropy and depolarization, by providing all the 16 elements of the 4 × 4 Mueller matrix in a single measurement [22–25]. In our previous work, we used an MME to measure the polarization parameters of an arbitrary composite wave plate, including the retardance, the fast-axis azimuth, and the rotary angle and accurately calibrated the misalignment errors in the composite wave plate from the oscillations in the spectra of these characteristic parameters [12]. As a continuation of our previous work, in this paper, we propose a method to accurately align the axes of an arbitrary biplate by detecting and minimizing the oscillations in the spectra of the characteristic parameters of the biplate using a spectroscopic MME. We construct an optical model to describe the biplate based on Jones's equivalent theorem [26] and derive analytical relations between the misalignment errors and the characteristic parameters of the biplate. This analytical model helps us to analyze the sensitivity of the characteristic parameters to the misalignment errors and evaluate the alignment accuracy and the residual misalignment errors quantitatively. We further present the principles of the proposed method to align the axes of the biplate using an MME. An experimental device based on a house-developed MME and a high-precision, automatic-rotation stage are described and set up to detect and control all the characteristic parameters of the biplate to be aligned. Experimental results on the alignment of a quartz biplate designed as a quarter-wave retarder at 632.8 nm demonstrate that the alignment accuracy of proposed method is better than 0.01°.

2. METHOD

A. Modeling of the Biplate

A wave plate is usually made from birefringent crystal, such as quartz or MgF_2, cut with the optic axis parallel to the surface of the plate. The retardance of the wave plate is given by

$$\delta = \frac{2\pi}{\lambda}\Delta n \cdot d, \tag{1}$$

where $\Delta n = (n_e - n_o)$ is the birefringence of the crystal, n_e and n_o denote the extraordinary and the ordinary refractive indices, and d and λ refer to the thickness of the wave plate and the vacuum wavelength, respectively.

A single wave plate can be treated as a linear retarder, whose effects on the polarized light can be represented by a 2 × 2 Jones matrix [26]. If we study the wave plate in a Cartesian coordinate system and assume the light propagates along the z axis and perpendicularly to the plane of the wave plate, the Jones matrix of the wave plate is given by

$$\mathbf{J}(\delta,\theta) = \begin{bmatrix} \cos(\delta/2)+\mathrm{i}\sin(\delta/2)\cos(2\theta) & \mathrm{i}\sin(\delta/2)\sin(2\theta) \\ \mathrm{i}\sin(\delta/2)\sin(2\theta) & \cos(\delta/2)-\mathrm{i}\sin(\delta/2)\cos(2\theta) \end{bmatrix}, \tag{2}$$

where i is the imaginary unit, and δ and θ are the retardance of the single wave plate and the azimuth of its fast axis with respect to the x axis, respectively.

A general biplate can be treated as an optical system consisting of two single wave plates. We again study the biplate in the Cartesian coordinate system, and the single wave plates are numbered as 1, 2 in the order of light propagation. Furthermore, let (d_i, θ_i) denote the thickness and the fast-axis azimuth of the i-th single wave plate, respectively. The retardance of the i-th wave plate δ_i can be calculated by Eq. (1). Thus the effect of the biplate on the polarized light can be calculated by

$$\mathbf{J} = \mathbf{J}(\delta_2,\theta_2)\mathbf{J}(\delta_1,\theta_1) = \begin{bmatrix} J_{11} & J_{12} \\ J_{21} & J_{22} \end{bmatrix}, \tag{3}$$

where $\mathbf{J}(\delta_i, \theta_i)$ is the Jones matrix of the i-th wave plate calculated by Eq. (2), and the matrix $\mathbf{J}$ is unitary and its elements are

$$J_{11} = J_{22}^* = l_0 + l_1, \tag{4a}$$

$$J_{12} = -J_{21}^* = l_2 - l_3, \tag{4b}$$

where the notation "*" represents the complex conjugate of a complex number, and $l_0 - l_3$ can be calculated as

$$l_0 = \cos\frac{\delta_2}{2}\cos\frac{\delta_1}{2} - \sin\frac{\delta_2}{2}\sin\frac{\delta_1}{2}\cos(2\theta_2 - 2\theta_1), \quad \textbf{(5a)}$$

$$l_1 = \mathrm{i}\left(\cos\frac{\delta_2}{2}\cos\frac{\delta_1}{2}\cos 2\theta_1 + \sin\frac{\delta_2}{2}\sin\frac{\delta_1}{2}\cos 2\theta_2\right), \quad \textbf{(5b)}$$

$$l_2 = \mathrm{i}\left(\cos\frac{\delta_2}{2}\cos\frac{\delta_1}{2}\sin 2\theta_1 + \sin\frac{\delta_2}{2}\sin\frac{\delta_1}{2}\sin 2\theta_2\right), \quad \textbf{(5c)}$$

$$l_3 = \sin\frac{\delta_2}{2}\sin\frac{\delta_1}{2}\sin(2\theta_2 - 2\theta_1). \quad \textbf{(5d)}$$

According to Jones's equivalent theorem, the biplate can be optically equivalent to a cascaded system containing a pure linear retarder and a rotator [26]. Therefore, the Jones matrix of the biplate can be described as

$$\mathbf{J} = \mathbf{R}(\rho_e)\mathbf{J}(\delta_e, \theta_e), \quad \textbf{(6)}$$

where (δ_e, θ_e) are the equivalent retardance and the equivalent fast-axis azimuth of the linear retarder, ρ_e is the rotary angle of the resulting rotator, and $\mathbf{R}(\rho_e)$ is the Jones rotation matrix of the rotator and is given by

$$\mathbf{R}(\rho_e) = \begin{bmatrix} \cos\rho_e & \sin\rho_e \\ -\sin\rho_e & \cos\rho_e \end{bmatrix}. \quad \textbf{(7)}$$

Combining Eqs. (3)–(7), we can derive the expressions of the equivalent parameters of the biplate shown as

$$\delta_e = 2\tan^{-1}\left[\sqrt{\frac{\mathrm{Im}^2(J_{11}) + \mathrm{Im}^2(J_{12})}{\mathrm{Re}^2(J_{11}) + \mathrm{Re}^2(J_{12})}}\right], \quad \textbf{(8a)}$$

$$\theta_e = \frac{1}{2}\tan^{-1}\left[\frac{\mathrm{Re}(J_{11})\mathrm{Im}(J_{12}) + \mathrm{Im}(J_{11})\mathrm{Re}(J_{12})}{\mathrm{Re}(J_{11})\mathrm{Im}(J_{11}) - \mathrm{Re}(u_{12})\mathrm{Im}(J_{12})}\right], \quad \textbf{(8b)}$$

$$\rho_e = \tan^{-1}\left[\frac{\mathrm{Re}(J_{12})}{\mathrm{Re}(J_{11})}\right]. \quad \textbf{(8c)}$$

Or,

$$\delta_e = 2\tan^{-1}\left(\sqrt{\frac{-l_1^2 - l_2^2}{l_0^2 + l_3^2}}\right), \quad \textbf{(9a)}$$

$$\theta_e = \frac{1}{2}\tan^{-1}\left(\frac{l_0 l_2 - l_1 l_3}{l_0 l_1 + l_2 l_3}\right), \quad \textbf{(9b)}$$

$$\rho_e = \tan^{-1}\left(\frac{-l_3}{l_0}\right). \quad \textbf{(9c)}$$

B. Alignment Principle

The biplate produces a compound zero-order retarder if the single wave plates are made of the same material. While, the biplate will produce an achromatic retarder if the single wave plates are made of different materials. In the design of an ideal biplate, the azimuthal angle between the fast axes of the two single wave plates is usually 90°. Practically, the biplate inevitably has axis-misalignment error between the single wave plates, as schematically shown in Fig. 1. In this case, the relation between the fast-axis azimuths of the single wave plates is

$$\theta_2 = \theta_1 + 90° + \alpha, \quad \textbf{(10)}$$

where α is the misalignment error between the fast axis of the second single wave plate and the slow axis of the first single wave plate in the biplate.

Generally, the axis-misalignment error of the single wave plates in the biplate is a small angle. In this case, we have $\sin\alpha \approx \alpha$ and $\cos\alpha \approx 1$ for the misalignment angle. Substituting Eqs. (10) and (5) into Eq. (9), we have

$$\delta_e \approx \delta_1 - \delta_2, \quad \textbf{(11a)}$$

$$\theta_e \approx \frac{1}{2}\tan^{-1}\left[-2\alpha\frac{\sin\delta_2}{\sin(\delta_1 - \delta_2)}\right] + \theta_1, \quad \textbf{(11b)}$$

$$\rho_e \approx \tan^{-1}\left[-2\alpha\frac{1}{\cot(\delta_1/2)\cot(\delta_2/2) + 1}\right]. \quad \textbf{(11c)}$$

For an ideal biplate, the misalignment error is zero, and the equivalent parameters are $\delta_e = \delta_1 - \delta_2$, $\theta_e = \theta_1$, and $\rho_e = 0$. Practically, since the retardances (δ_1, δ_2) are wavelength dependent due to the dispersive birefringence of the material, the equivalent parameters of the biplate shown in Eq. (11) are thereby functions of wavelength when the misalignment error is not zero. From Eq. (11), we can see that the equivalent fast-axis azimuth and the equivalent rotary angle are much more sensitive to the misalignment error than the equivalent retardance. Here we define two amplitude parameters for the equivalent fast-axis azimuth and the equivalent rotary angle over a spectral range as follows:

$$A_\theta(\alpha) = \max_{\lambda\in\Gamma}[\theta_e(\lambda)] - \min_{\lambda\in\Gamma}[\theta_e(\lambda)], \quad \textbf{(12a)}$$

$$A_\rho(\alpha) = \max_{\lambda\in\Gamma}[\rho_e(\lambda)] - \min_{\lambda\in\Gamma}[\rho_e(\lambda)], \quad \textbf{(12b)}$$

where $\mathbf{\Gamma}$ is the spectral range to be concerned.

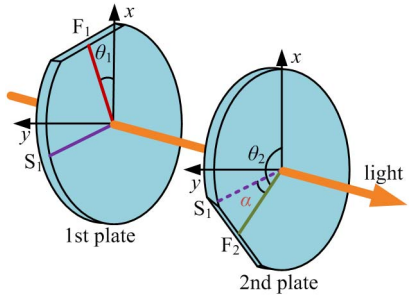

Fig. 1. Scheme of a general biplate. S_1 is the slow axis of the first wave plate, and (F_i, θ_i) $(i = 1, 2)$ denote the fast axis of the i-th wave plate and its azimuth with respect to the x axis; α denotes the angular misalignment error between the fast axis of the first wave plate and the slow axis of the second wave plate.

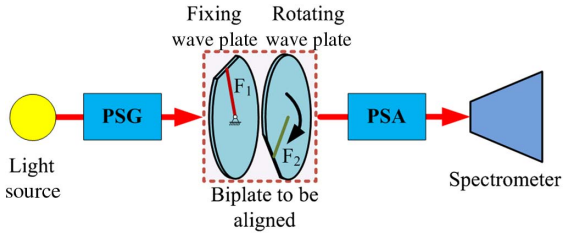

Fig. 2. Scheme of the experimental setup for alignment of the biplate based on the MME. PSG, polarization state generator; PSA, polarization state analyzer; F_1, fast axis of first single wave plate; F_2, fast axis of second single wave plate.

From Eq. (11), it can be seen that there are positive correlations between the amplitude parameters and the absolute misalignment error of the biplate. Inspired by this point, we can use the equivalent fast-axis azimuth or the equivalent rotary angle as the detected parameter to accurately align the axes of the biplate.

In this paper, we use a spectroscopic MME in the straight-through mode to measure all the equivalent parameters of the biplate and then accurately align its axes. As schematically shown in Fig. 2, the biplate to be aligned is treated as the sample and placed between the polarization state generator (PSG) and the polarization state analyzer (PSA) of the MME. One single wave plate of the biplate is fixed, and the other one can be rotated with respect to the fixing wave plate. The MME can be operated over a wide spectral range by using a spectrometer as the detector, a wide spectral light source, and other achromatic elements [27]. The characteristic parameter spectra of the biplate, including the equivalent fast-axis azimuth, the equivalent rotary angle, as well as the equivalent retardance, can be extracted from its Muller matrix measured by the MME [12].

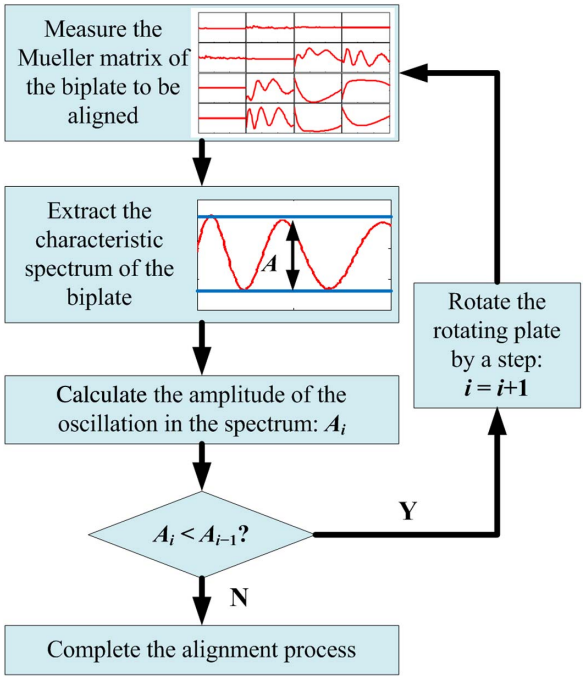

Fig. 3. Flow chart of alignment procedure for the biplate using MME.

Since the equivalent retardance of the biplate is not sensitive to the misalignment error, we can choose either the equivalent fast-axis azimuth or the equivalent rotary angle as the characteristic parameter to guide the alignment procedure. The aim of the alignment procedure is to control the amplitude parameter of the oscillations in the chosen detected spectrum (i.e., the equivalent fast-axis azimuth or the equivalent rotary angle) to the minimum by rotating one single wave plate with respect to the other one. The flow chart of the alignment procedure for the biplate using MME is shown in Fig. 3. In practice, we can use a method combining coarse and fine alignment to make the alignment procedure more efficient. The coarse alignment has a larger rotation step, which aims to locate a rough range for the alignment position, while the fine alignment has a smaller rotation step, which aims to locate the accurate alignment position and complete the alignment procedure.

3. EXPERIMENTAL SETUP

Figure 4 shows the prototype of the experimental setup based on a house-developed broadband MME consisting of a light source, a PSG, a sample stage, a PSA, and a detector [22,27]. The PSG contains a polarizer followed by a rotating compensator, while the PSA contains a second rotating compensator followed by an analyzer. In the device, the light source is a deuterium and quartz-tungsten-halogen-combined source, the polarizer and the analyzer are α-BBO Rochon prisms, and the detector is a commercial spectrometer. The rotating compensators are house-designed achromatic retarders, which contain three quarter-wave plates made of quartz with optimized central wavelengths and axis orientations [27]. With the components used in the house-developed MME, the available wavelength range covers 200–1000 nm. Two measurement modes, named as the straight-through measurement mode and the reflective measurement mode, can be chosen by rotating the PSG arm and the PSA arm of the ellipsometer simultaneously. In this paper, the alignment experiments of the biplate are performed in the straight-through measurement mode.

The house-developed MME has been set up with a strict system calibration to ensure the performances in the measurement of the Mueller matrix. The system calibration aims to determine the systematic parameters of the ellipsometer, including the retardances of the compensators, the orientations of the polarized components, and some imperfections in the system, and this is done by a regressive iteration procedure using a standard calibration sample at the reflective measurement mode [27,28]. With the calibration of the systematic parameters and corrections of the imperfections in the system such as depolarization artifacts, the total deviations, including the systematic errors and the measurement noises in the Mueller matrix elements from their nominal values, are less than ± 0.002 over the whole applicable spectral range [27,29].

The biplate to be aligned is mounted on a high-precision, automatic-rotation stage from OptoSigma controlled by a single-axis controller from OptoSigma with the highest resolution of 0.0025°. As shown in Fig. 4, both of the single wave

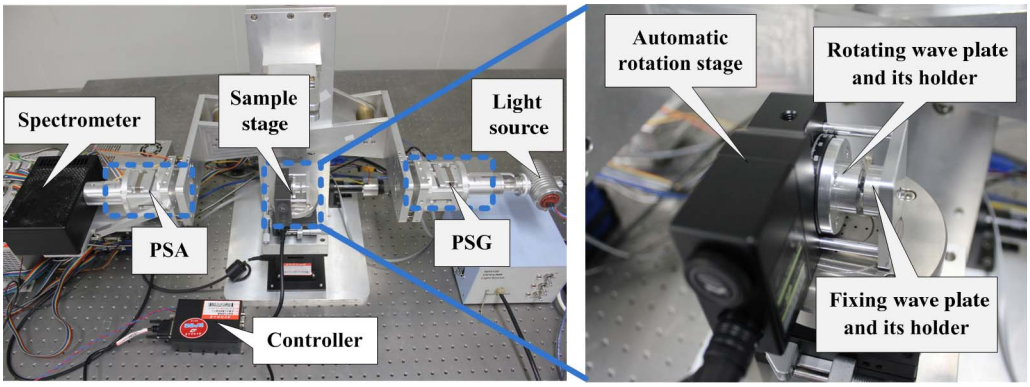

Fig. 4. Prototype of the experimental setup based on a house-developed MME and a high-precision, automatic-rotation stage for the alignment of optical axes of the biplate.

plates of the biplate are mounted in protective holders and then connected to the stage. One of them is connected to the turntable of the stage and can be rotated with the turntable, while the other one is connected to the base of the stage and remains stationary during the rotation. The biplate to be aligned is mounted in the rotation stage and then placed on the sample stage of the MME, where it is attentively adjusted to ensure the light spot totally propagates through the biplate at normal incidence. A computer is connected with both the controller and ellipsometer to control the rotation stage and complete the data analysis.

4. RESULTS AND DISCUSSION

A quartz biplate, which is designed as a compound zero-order, quarter-wave plate at 632.8 nm, is taken as an example to verify the proposed method. The single wave plates of the biplate are supplied by Wuhan Union Optics with their fast axes roughly marked. The thicknesses of the single wave plates are 0.384 mm and 0.402 mm. Since the optical activity in the quartz crystal has significant influence on the rotary angle, we chose the fast-axis azimuth as the characteristic parameter for the alignment of the quartz biplate in this paper. The single wave plates are mounted on the rotation stage with their fast axes roughly perpendicular to each other according to the axis markers provided by the supplier. The alignment is performed according to the flow chart shown in Fig. 3, and the rotation steps for coarse alignment and fine alignment are 0.5° and 0.01°, respectively. For each step of the rotation, the MME measures the characteristic parameter spectra of the biplate, and the experimental results are shown in Figs. 5–7 and Table 1.

Figure 5 shows the experimental results of the fast-axis azimuth over the spectral range of 550–750 nm versus the rotation angles of the stage. In Fig. 5, obvious quasi-periodic oscillations are observed in the fast-axis azimuth spectra, which can be assigned to the angular misalignment errors between the single wave plates of the biplate as described in Section 2. The periods of these oscillations increase with the wavelength, but they remain unchanged during the rotation of the alignment. The amplitudes of these oscillations first decrease with the rotation and then increase with the rotation. As described in Section 2, the alignment position of the biplate locates at

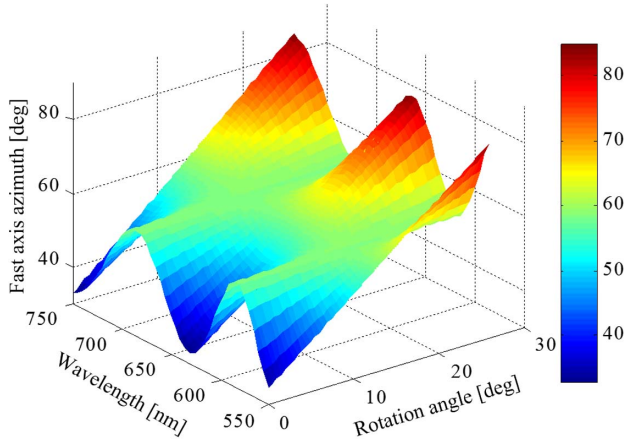

Fig. 5. Fast-axis azimuth spectra of the quartz biplate versus the rotation angle.

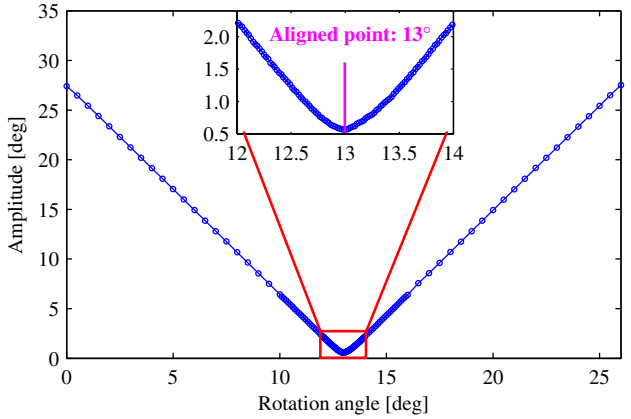

Fig. 6. Amplitude parameters of the oscillations in the fast-axis azimuth spectra versus the rotation angle.

the turning point of the oscillation amplitude, i.e., the minimum of the amplitude.

To clearly find the alignment position of the biplate, we calculate the amplitude parameters of the oscillations in the fast-axis azimuth spectra over the wavelength range of 550–750 nm

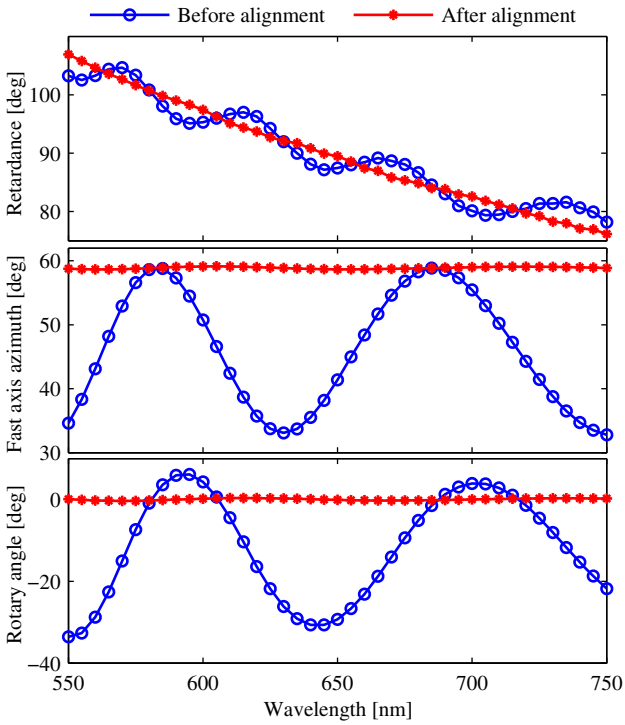

Fig. 7. Equivalent parameter spectra of the biplate before and after the alignment.

according to Eq. (12a) and then plot them against the rotation angle as shown in Fig. 6. It can be seen from Fig. 6 that there is an approximate linear relationship between the amplitude parameter of the oscillations and the misalignment error in the biplate, and the curve obviously exhibits opposite monotonicity before and after the minimum point, which makes it convenient for us to distinguish the alignment position. From Fig. 6, it can be clearly observed that the amplitude first decreases and then increases with the rotation, and the minimum amplitude occurs at the rotation of 13.00°, which is judged as the alignment position of the biplate. The misalignment error increases when rotating toward both sides before and after the alignment position.

Figure 7 shows the comparison of the equivalent parameter spectra of the biplate before and after the axis alignment. All of the equivalent parameter spectra exhibit obvious quasi-periodic oscillations before alignment because the biplate contains large misalignment errors ($|\alpha| \approx 13.00°$). In addition, the amplitudes of the oscillations in the fast-axis azimuth and the rotary-angle spectra are of the same order of magnitude and more than one order larger than those in the retardance spectra, which thereby indicates that the retardance is not as sensitive to the misalignment error as it is to the fast-axis azimuth and the rotary angle. All the oscillations in these equivalent parameter spectra nearly disappeared after the alignment procedure, which verifies the proposed method for the alignment of biplate. To further explore the alignment precision and accuracy of the proposed method, we repeat the alignment procedure 10 times with the rotation angle ranging from 12° to 14° with a rotation step of 0.01°. The experimental results of the alignment positions are recorded in Table 1. Here we use the maximum deviation from the mean value and the standard deviation of the alignment positions to evaluate the accuracy and the precision of the alignment method. According to Table 1, the mean value, the maximum deviation, and the standard deviation of the 10 alignment positions are 12.997°, 0.007°, and 0.005°, respectively. Thus we can conclude that the accuracy and the precision of the proposed method are both better than 0.01° in the axis alignment of a biplate.

Due to the lack of an analytical model, the reported techniques only reduced the deviations in the chosen characteristic parameters below detectability, but they did not give quantitative assessment of the alignment accuracy [20,21]. It can be roughly known from the published literatures that the residual misalignment errors in the wave plates from producers (e.g., B-halle, Thorlabs, J. Fichou, and Wuhan Union Optics) are larger than 0.1° [5,11,12,15]. Based on this point, we conclude that the presented method significantly improves the axis alignment accuracy and can further quantitatively evaluate the alignment accuracy and residual misalignment errors.

The accuracy and precision of the proposed alignment method are determined by the measurement accuracy and precision of the fast-axis azimuth and the resolution of the rotation stage. In the experiment, we also set smaller rotation steps (e.g., 0.005°) to attempt to improve the alignment accuracy. However, in this case, the difference between the oscillation amplitudes of two adjacent rotation positions is smaller than the level of noises in the fast-axis azimuth. Thus the alignment accuracy of the presented alignment procedure depends on the detectability of the MME. The limitation of the alignment accuracy is about 0.01°. Higher alignment accuracy requires improvements in the measurement accuracy and precision of the fast-axis azimuth of the biplate.

In addition, it is also worth pointing out that the axis alignment method presented in this paper can be easily extended to align the optical axes of more complex composite wave plates consisting of more single wave plates whose fast axes are designed to be perpendicular or parallel to each other, such as achromatic wave plates made of different birefringent materials. In this case, two single wave plates of the composite wave plate are treated as a biplate and aligned first, and then the aligned single wave plates are treated as a whole and aligned with another single wave plate until all the single wave plates are aligned accurately.

Table 1. Experimental Results of 10 Repeated Alignment Procedures for the Quartz Biplate Performed on the House-Developed MME

Exp. No.	1	2	3	4	5	6	7	8	9	10
Alignment Position (°)	13.00	13.00	12.99	13.00	13.00	12.99	13.00	12.99	13.00	13.00

5. CONCLUSIONS

In this paper, we propose a spectral method to accurately align the axes of the single wave plates of a biplate. In the alignment procedure, we detected the characteristic parameter spectra of the biplate using an MME and controlled the oscillations in the detected spectra to a minimum by rotating one single wave plate with respect to the other one. We construct an optical model based on Jones's equivalent theorem to describe a general biplate and to present the principle of the alignment method. Analytical relations between the equivalent parameters and the misalignment error are derived. We find that the fast-axis azimuth and the rotary angle of the biplate are much more sensitive to the misalignment error than the retardance. Two amplitude parameters for the equivalent fast-axis azimuth and the equivalent rotary angle over a spectral range are defined to guide the alignment procedure. An experimental device based on a house-developed MME is set up to detect the characteristic parameter spectra of the biplate and perform the alignment procedure. In the experiments, a high-precision, automatic-rotation stage is applied to rotate one single wave plate with respect to the other one of the biplate. Experimental results demonstrate that the alignment accuracy of the proposed method is better than 0.01° in aligning a quartz biplate, which is designed as a zero-order, quarter-wave retarder for 632.8 nm. The proposed method has the advantage of high accuracy, precision, and quantitative characterization when compared with previously published techniques.

Funding. National Natural Science Foundation of China (NSFC) (51475191, 51405172, 51575214, 51525502); Natural Science Foundation of Hubei Province of China (2015CFB278, 2015CFA005); China Postdoctoral Science Foundation (2015T80791); and Program for Changjiang Scholars and Innovative Research Team in University of China (IRT13017).

Acknowledgment. H. Gu is thankful for the support from the Graduates' Innovation and Entrepreneurship Fund of Huazhong University of Science and Technology and the efforts and useful discussions in the experiments from Mr. Shuai Ren, who was an undergraduate student at Huazhong University of Science and Technology until July, 2015.

REFERENCES

1. J. Li, B. Ramanujam, and R. W. Collins, "Dual rotating compensator ellipsometry: theory and simulations," Thin Solid Films **519**, 2725–2729 (2011).
2. D. E. Aspnes, "Spectroscopic ellipsometry—past, present, and future," Thin Solid Films **571**, 334–344 (2014).
3. P. A. Williams, "Rotating-wave-plate Stokes polarimeter for differential group delay measurements of polarization-mode dispersion," Appl. Opt. **38**, 6508–6515 (1999).
4. M. P. Kothiyal and C. Delisle, "Shearing interferometer for phase shifting interferometry with polarization phase shifter," Appl. Opt. **24**, 4439–4442 (1985).
5. C. Hu, L. Sun, J. M. Flores-Camacho, M. Hohage, C. Liu, X. Hu, and P. Zeppenfeld, "A rotating-compensator based reflectance difference spectrometer for fast spectroscopic measurements," Rev. Sci. Instrum. **81**, 043108 (2010).
6. J. F. de Boer and T. E. Milner, "Review of polarization sensitive optical coherence tomography and Stokes vector determination," J. Biomed. Opt. **7**, 359–371 (2002).
7. J. M. Beckers, "Achromatic linear retarders," Appl. Opt. **10**, 973–975 (1971).
8. P. D. Hale and G. W. Day, "Stability of birefringent linear retarders (waveplates)," Appl. Opt. **27**, 5146–5153 (1988).
9. E. A. West and M. H. Smith, "Polarization errors associated with birefringent waveplates," Opt. Eng. **34**, 1574–1580 (1995).
10. D. B. Chenault and R. A. Chipman, "Measurements of linear diattenuation and linear retardance spectra with a rotating sample spectropolarimeter," Appl. Opt. **32**, 3513–3519 (1993).
11. Z. Han, Z. Xu, and L. Chen, "A three-spectrum method for accurate calibration of bi-plate zero-order retarder," Chin. Opt. Lett. **12**, 031202 (2014).
12. H. Gu, S. Liu, X. Chen, and C. Zhang, "Calibration of misalignment errors in composite waveplates using Mueller matrix ellipsometry," Appl. Opt. **54**, 684–693 (2015).
13. K. Ebert and D. E. Aspnes, "Biplate artifacts in rotating-compensator ellipsometers," Thin Solid Films **455**–456, 779–783 (2004).
14. P. Marsik and J. Humlicek, "Multi-plate misalignment artifacts in rotating-compensator ellipsometry: analysis and data treatment," Phys. Status Solidi C **5**, 1064–1067 (2008).
15. B. Boulbry, B. Bousquet, B. L. Jeune, Y. Guern, and J. Lotrian, "Polarization errors associated with zero-order achromatic quarter-wave plates in the whole visible spectral range," Opt. Express **9**, 225–235 (2001).
16. H. Dong, M. Tang, and Y. D. Gong, "Measurement errors induced by deformation of optical axes of achromatic waveplate retarders in RRFP Stokes polarimeters," Opt. Express **20**, 26649–26666 (2012).
17. H. Dai and C. Yan, "Measurement errors resulted from misalignment errors of the retarder in a rotating-retarder complete Stokes polarimeter," Opt. Express **22**, 11869–11883 (2014).
18. B. Boulbry, B. L. Jeune, F. Pellen, J. Cariou, and J. Lotrian, "Identification of error parameters and calibration of a double-crystal birefringent wave plate with a broadband spectral light source," J. Phys. D **35**, 2508–2515 (2002).
19. G. Cui, G. Li, X. Guo, T. Liu, and Y. Chen, "Calibration of the MgF_2 biplate compensator using a straight-through ellipsometer," in *Third International Conference on Instrumentation, Measurement, Computer, Communication and Control (IMCCC)* (IEEE, 2013), pp. 731–735.
20. D. E. Aspnes, "Alignment of an optically active biplate compensator," Appl. Opt. **10**, 2545–2546 (1971).
21. J. Lee, P. I. Rovira, I. An, and R. W. Collins, "Alignment and calibration of the MgF_2 biplate compensator for applications in rotating-compensator multichannel ellipsometry," J. Opt. Soc. Am. A **18**, 1980–1985 (2001).
22. S. Liu, X. Chen, and C. Zhang, "Development of a broadband Mueller matrix ellipsometer as a powerful tool for nanostructure metrology," Thin Solid Films **584**, 176–185 (2015).
23. X. Chen, S. Liu, C. Zhang, H. Jiang, Z. Ma, T. Sun, and Z. Xu, "Accurate characterization of nanoimprinted resist patterns using Mueller matrix ellipsometry," Opt. Express **22**, 15165–15177 (2014).
24. X. Chen, C. Zhang, S. Liu, H. Jiang, Z. Ma, and Z. Xu, "Mueller matrix ellipsometric detection of profile asymmetry in nanoimprinted grating structures," J. Appl. Phys. **116**, 194305 (2014).
25. X. Chen, Y. Shi, H. Jiang, C. Zhang, and S. Liu, "Nondestructive analysis of lithographic patterns with natural line edge roughness from Mueller matrix ellipsometric data," Appl. Surf. Sci., doi: (to be published).
26. H. Hurwitz, Jr. and R. C. Jones, "A new calculus for the treatment of optical systems. Part II. Proof of three general equivalence theorems," J. Opt. Soc. Am. **31**, 493–499 (1941).
27. H. Gu, X. Chen, H. Jiang, C. Zhang, and S. Liu, "Optimal broadband Mueller matrix ellipsometer using multi-waveplates with flexibly oriented axes," J. Opt. **18**, 025702 (2016).
28. B. Johs, "Regression calibration method for rotating element ellipsometers," Thin Solid Films **234**, 395–398 (1993).
29. W. Li, C. Zhang, H. Jiang, X. Chen, and S. Liu, "Depolarization artifacts in dual rotating-compensator Mueller matrix ellipsometry," J. Opt. **18**, 055701 (2016).